Results in Engineering 27 (2025) 105870

Contents lists available at ScienceDirect

Results in Engineering

journal homepage: www.sciencedirect.com/journal/results-in-engineering

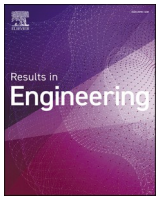

Research paper

Numerical evaluation of a dual phase change material-integrated cap for prolonged thermal protection in extreme heat

Mohammad Junaid [a], Goutam Saha [b,c,*], Pabel Shahrear [d], Suvash C. Saha [e,*]

[a] Department of Mechanical Engineering, Shahjalal University of Science and Technology, Sylhet 3114, Bangladesh
[b] Department of Mathematics, University of Dhaka, Dhaka 1000, Bangladesh
[c] Miyan Research Institute, International University of Business Agriculture and Technology, Uttara, Dhaka 1230, Bangladesh
[d] Department of Mathematics, Shahjalal University of Science and Technology, Sylhet, 3114, Bangladesh
[e] School of Mechanical and Mechatronic Engineering, Faculty of Engineering and Information Technology, University of Technology Sydney, Sydney, NSW, Australia

ARTICLE INFO

Keywords:
Phase change material (PCM)
Heat protective cap
Enthalpy-porosity method
Wearable cooling device
Passive thermal management

ABSTRACT

With the increasing frequency of extreme heat events, effective thermal regulation in wearable caps is essential. This study presents a numerical investigation of a PCM-integrated wearable cap designed for prolonged outdoor exposure. Two PCMs—Rubitherm RT-27 and Capric Acid—were analyzed under natural convection for their temperature control, melting behavior, and energy storage capacity. At an ambient temperature of 40 °C, RT-27 achieved full melting in 155 min, while Capric Acid required 230 min, offering extended thermal protection. At 50 °C, melting times reduced to 108 min for RT-27 and 133 min for Capric Acid. The dual-PCM system maintained inner cap temperatures between 6 and 14 °C lower than ambient, depending on the PCM and external conditions. RT-27 provided rapid initial cooling, whereas Capric Acid ensured sustained thermal regulation. The cap's layered design, including wool-cotton insulation, further delayed heat transfer and enhanced comfort. Compared to conventional fabric-based caps, the PCM-integrated cap significantly prolonged thermal relief duration. This study demonstrates the practical potential of multi-PCM systems for wearable passive cooling applications in extreme environments.

1. Introduction

The increasing frequency and intensity of extreme heat events, driven by climate change and urbanization, have amplified the demand for efficient thermal protection strategies. These extreme conditions pose significant challenges to various systems, structures, and individuals, necessitating innovative solutions to mitigate heat-related risks [1]. Among the various strategies investigated, incorporating Phase Change Materials (PCMs) has proven to be a highly effective thermal management technique, leveraging their capacity to absorb and release latent heat during phase transitions [2]. This characteristic makes PCM particularly effective in applications requiring thermal regulation, especially in environments exposed to fluctuating or high temperatures. Thermal protective systems, such as caps, helmets, and other wearable gear, play a critical role in safeguarding individuals working in harsh environments, including firefighters, military personnel, athletes, and outdoor laborers. However, the performance of these systems is often limited by their inability to provide consistent thermal insulation under varying convective heat transfer conditions. Natural convection, forced convection, and mixed convection each present unique challenges, as they influence heat transfer rates and thermal gradients differently. Some of the following relevant literature are presented hereafter:

Wang et al. [3] investigated factors affecting PCM performance in cooling clothing, such as phase-change temperature, composition, and placement. They found that optimizing these properties enhances heat dissipation, reduces microenvironment temperature and humidity, and improves thermal comfort. Mondal [4] reviewed the integration of PCMs into textiles and their applications, focusing on methods such as microencapsulation, coating, and lamination to incorporate PCMs into fabrics for thermal regulation. The study found that PCM-incorporated textiles effectively enhanced thermal comfort by storing and releasing heat during phase transitions, making them suitable for applications in smart clothing, bedding, and protective garments. Wang et al. [5] experimentally tested PCM-integrated firefighters' gloves for thermal protection. They observed that a 1-mm-thick PCM layer extended protection time by up to five times, with a 68 °C melting point PCM offering

* Corresponding authors.
E-mail addresses: gsahamath@du.ac.bd (G. Saha), shahrear-mat@sust.edu (P. Shahrear), Suvash.Saha@uts.edu.au (S.C. Saha).

https://doi.org/10.1016/j.rineng.2025.105870
Received 26 March 2025; Received in revised form 28 May 2025; Accepted 18 June 2025
Available online 19 June 2025

Nomenclature

Symbols

C_p	Specific heat (kJ/kg K)
g_x	Gravitational acceleration along X-axis (m/s^2)
g_y	Gravitational acceleration along Y-axis (m/s^2)
g_z	Gravitational acceleration along Z-axis (m/s^2)
k	Thermal conductivity (W/m K)
P	Pressure (Pa)
T	Temperature (°C)
T_∞	Ambient temperature (°C)
T_{skin}	Skin temperature (°C)
T_m	Melting point (°C)
T_l	Liquidus temperature (°C)
T_s	Solidus temperature (°C)
L_h	Latent heat of fusion (kJ/kg)
h	Sensible enthalpy (kJ/kg)
H	Total enthalpy (kJ/kg)
ΔH	Latent heat (kJ/kg)
Q	Heat flux (W/m^2)
A_{mush}	Mushy zone constant (kg/m^3 s)
u	Velocity along X-axis (m/s)
v	Velocity along Y-axis (m/s)
w	Velocity along Z-axis (m/s)
t	Time (s)

Greek letters

γ	Liquid fraction
μ	Dynamic viscosity (kg/m s)
ρ	Density solid/liquid (kg/m^3)
β	Thermal expansion coefficient (1/K)
ε	A small number (0.001) used to avoid division by zero

Subscript

PCM	Phase change material
l	Liquid
s	Solid

optimal performance depending on placement. Omara et al. [6] systematically reviewed the application of PCMs in helmets for cooling involves evaluating designs, materials, and performance aspects. The study found that PCMs effectively maintain comfort temperatures but face challenges like ventilation issues and moisture condensation, with potential improvements through active systems and optimized designs. Nagaraju et al. [7] numerically evaluate the thermal performance of two-PCMs (RT27 and Capric acid) within a thermal energy storage (TES) system designed for helmet cooling, considering factors like PCM orientation, latent heat, and melting behavior. They found that RT27 provided better cooling performance with faster melting times (150 min compared to 175 min for Capric acid) and greater air temperature reduction when the PCM packet was oriented horizontally, making it more effective for microclimate cooling applications.

Tan and Fok [8] designed a helmet cooling system incorporating PCM enclosed in a pouch positioned between the helmet and the wearer's head. Heat was transferred via conduction through a heat collector, maintaining the head temperature slightly above the PCM temperature without the need for electrical power. The system provided comfort cooling for up to two hours, and the PCM could be re-solidified for reuse by immersing the pouch in water for about 15 min. Reddy and Reddy [9] designed and analyzed a motorcycle helmet cooling system using PCMs, specifically salt hydrate PCM series S25 and S27, to absorb heat and provide thermal comfort. The study found that S25, with a higher melting temperature of 36 °C, provided longer cooling durations (up to 4.99 h) compared to S27, making it more suitable for maintaining comfort in helmets under hot conditions. Ghani et al. [10] utilized experimental and computational methods, including a 3D model, to examine the thermal performance of industrial helmets integrated with PCM and forced convection under various environmental conditions. The study found that the PCM pad maintained a constant temperature of 24 °C for over two hours, significantly improving thermal comfort by reducing helmet surface and skin temperatures, while forced convection reduced the maximum temperature near the user's head by approximately 10 °C. Ali et al. [11] integrated nano-graphene-paraffin composite PCM into safety helmets to enhance thermal conductivity and provide passive cooling. The study found that the composite improved thermal conductivity by 146 % (concentration = 3 %) and offered over four hours of thermal comfort at 35 °C. Venugopal et al. [12] enhanced Neopentylglycol (NPG) PCM with 0.1 % CuO, Al_2O_3, and TiO_2 nanoparticles to improve thermal conductivity, analyzed via DSC, TGA, FTIR, and T-history methods. Among these, NPG + 0.1 % CuO showed the best performance, with a 14.67 % conductivity increase and a 20 % reduction in helmet interior temperature, improving thermal comfort.

Sinnappoo et al. [13] explored the use of sustainable paraffinic PCMs as a textile liner inside motorcycle helmets to reduce heat stress. They evaluated the thermal performance of these materials using wind tunnel experiments and differential scanning calorimetry. They observed that PCM materials reduced the helmet's internal temperature by up to 3.8 °C and absorbed sufficient heat (up to 17.8 W) to alleviate heat stress, offering a practical solution for improving comfort without compromising helmet safety. Al-Rjoub et al. [14] developed a portable head cooling system using PCM and a helical heat exchanger for enhanced heat transfer. Their system successfully managed a 40 W heat load for 100 min, demonstrating its effectiveness for thermal regulation in high-heat conditions. Similarly focusing on wearable solutions, Jun et al. [15] tested the heat and moisture transfer properties of cap fabrics and evaluated subjective wearing sensations. They observed that water absorption and thermal conductivity significantly influenced internal temperature and comfort, with high water absorbency effectively lowering temperatures.

Despite extensive research on PCM integration in helmets and protective garments, limited studies have investigated their application in lightweight, flexible caps designed for extended wear in extreme heat environments. Most existing work focuses on rigid headgear with forced or mixed convection cooling mechanisms [6,7,15], leaving a gap in understanding PCM performance in naturally convective environments within soft textile-based headwear. The novelty of this work lies in the integration and optimization of two distinct PCMs (RT-27 and Capric Acid) in a textile-based wearable cap using a numerical simulation approach, which has not been addressed in prior literature.

1.1. Novelty of the study

Existing research on thermal regulation using PCMs has primarily focused on helmets, with limited attention given to lightweight caps designed to protect the head from extreme heat. This research gap highlights the need for innovative solutions to enhance head protection and thermal comfort in diverse conditions. To address these challenges, this study explores the incorporation of PCMs into thermal protective caps as a novel solution. By enabling dynamic thermal regulation and improved heat dissipation, this approach seeks to overcome the limitations of current designs, such as inadequate ventilation and limited performance across varying temperature ranges. Existing PCM applications have largely been confined to building materials and electronic cooling, with relatively few studies investigating their integration into

wearable systems.

This research aims to optimize the performance of Phase Change Materials (PCMs) such as Rubitherm RT-27 and Capric Acid, under natural convection by analyzing temperature distribution, liquid fraction evolution, and total energy storage. The goal is to ensure effective functionality across a broad temperature range. The development of a lightweight, flexible, and efficient cap for heat protection would provide a practical and versatile solution for individuals exposed to extreme heat conditions. Such advancements would fill a significant gap in the market, benefiting workers, athletes, and others who require effective thermal protection in demanding environments.

2. Physical model

The physical model developed in this study represents a three-dimensional (3D) spherical cap designed for thermal regulation. The cap consists of three distinct layers: the upper layer, middle layer, and bottom layer. Both the upper and bottom layers are made of a wool and cotton mixture fabric, while the middle layer is composed of PCM to enhance thermal performance. Additionally, the frontal part of the cap is constructed using the same wool and cotton mixture fabric as the upper and bottom layers. The cap has a diameter (D) of 18 cm, shown in Fig. 1, and the geometric properties of its various components, including thickness, surface area, and volume, are summarized in Table 1.

Upper Layer (Fig. 1a): The outermost layer of the cap, exposed to varying environmental conditions such as ambient temperature, wind, and humidity. This layer is designed to provide protection and insulation. Middle Layer (PCM) (Fig. 1b): The core layer of the cap, consisting of PCM, plays a critical role in thermal energy storage and release. The PCM absorbs heat during phase transitions (e.g., melting) and releases heat during solidification, ensuring consistent thermal comfort. Bottom Layer (Fig. 1c): The innermost layer of the cap, which is in direct contact with the head skin. This layer is designed to provide comfort and facilitate heat transfer between the head and the PCM layer. Frontal Part: A separate section of the cap, also made of a wool and cotton mixture fabric, providing additional coverage and insulation for the forehead region. The physical domain of the cap, including its layered structure and dimensions, is illustrated in Fig. 1. This schematic highlights the spatial distribution of the layers and the overall design of the cap. The upper surface of the cap is exposed to external environmental conditions, including ambient temperature and potential heat loss due to convection and radiation. The inner surface of the cap is in contact with the head skin, where heat transfer occurs via convection and conduction. The thermal interaction between the head and the cap is critical for the model's performance. No boundary condition was applied to the frontal part because its position is outside the head, and this approach also helps to reduce the complexity of the simulation. The material properties of each layer, such as thermal conductivity, specific heat capacity, and density, are essential for analyzing the thermal behavior of the cap. These properties are summarized in Table 2. The combination of the wool and cotton mixture fabric and PCMs ensures a balance between insulation, comfort, and thermal regulation.

Table 1
Geometric properties of the cap.

Layers	Thickness (mm)	Area (mm^2)	Volume (mm^3)
Upper	0.5	65,338	16,276
PCM	3	63,063	106,850
Bottom	0.5	57,409	14,266
Frontal Part	2	23,782	16,827

3. Mathematical modelling

The enthalpy-porosity method is a widely used numerical approach for simulating phase change processes in PCMs, particularly during melting and solidification. It employs the liquid fraction (γ), a dimensionless variable ranging from 0 (solid) to 1 (liquid), to represent the phase transition. Intermediate values ($0< \gamma <1$) indicate partially melted states where solid and liquid phases coexist [7,17].

The method integrates γ into the energy conservation equation, using enthalpy to account for both sensible and latent heat during phase change. It also modifies the momentum equations by introducing a porosity term, which reduces fluid velocity in regions where the material remains solid, simulating resistance to flow. A key advantage of this method is its ability to implicitly capture the phase interface through

Table 2
Physical properties of different types of PCM [16–18].

Properties	Wool and Cotton Mixture	Rubitherm RT-27	Capric Acid
Density solid/liquid, ρ (kg/m^3)	1425	880/790	1018/888
Specific heat C_p solid/liquid, (J/kg K)	1285	1800/2400	1900/2400
Thermal conductivity solid/liquid, k (W/mK)	0.18	0.15/0.24	0.372/0.153
Dynamic viscosity, μ (kg/ms)	N/A	0.00342	0.003125
Latent heat of fusion, L_h (kJ/kg)	N/A	179	152.7
Solidus temperature, T_s (°C)	24	24	24
Liquidus temperature, T_l (°C)	N/A	29	32

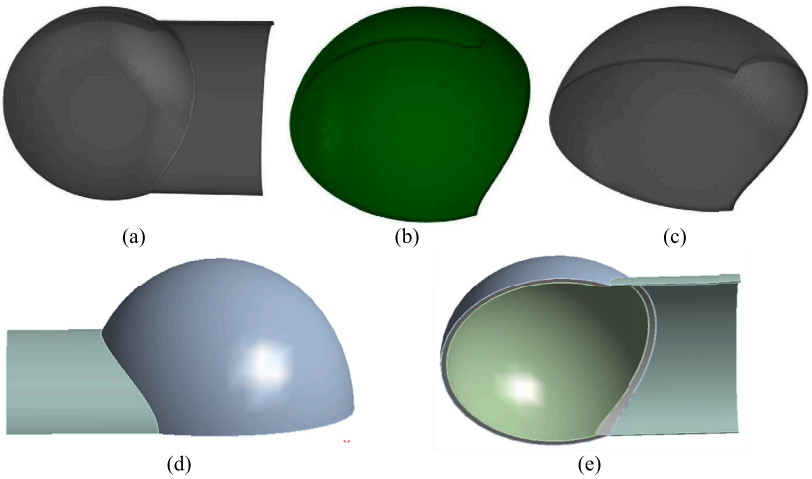

Fig. 1. Physical domain of a CAP: (a) upper layer plus frontal part, (b) inner layer, (c) bottom layer, (d) and (e) PCM integrated cap's outer and inner views.

variations in γ, avoiding the need to explicitly track the moving boundary. This simplifies computations while accurately modeling the thermal and flow behavior of PCMs. Its robustness and efficiency make it widely applied in research and engineering for phase change simulations [7,17,19].

Continuity Equation [7,17,19]:

$$\frac{\partial \rho}{\partial t}+\frac{\partial(\rho u)}{\partial x}+\frac{\partial(\rho v)}{\partial y}+\frac{\partial(\rho w)}{\partial z}=0 \tag{1}$$

Momentum Equations [7,17,19]:

$$\frac{\partial}{\partial t}(\rho u)+u\frac{\partial(\rho u)}{\partial x}+v\frac{\partial(\rho u)}{\partial y}+w\frac{\partial(\rho u)}{\partial y}=-\frac{\partial p}{\partial x}+\mu\nabla^2 u+\rho\beta\vec{g}_x(T-T_{ref})+\frac{(1-\gamma)^2}{(\gamma^3+\varepsilon)}A_{mush}u \tag{2}$$

$$\frac{\partial}{\partial t}(\rho v)+u\frac{\partial(\rho v)}{\partial y}+v\frac{\partial(\rho v)}{\partial y}+w\frac{\partial(\rho v)}{\partial y}=-\frac{\partial p}{\partial y}+\mu\nabla^2 v+\rho\beta\vec{g}_y(T-T_{ref})+\frac{(1-\gamma)^2}{(\gamma^3+\varepsilon)}A_{mush}v \tag{3}$$

$$\frac{\partial}{\partial t}(\rho w)+u\frac{\partial(\rho w)}{\partial z}+v\frac{\partial(\rho w)}{\partial z}+w\frac{\partial(\rho w)}{\partial z}=-\frac{\partial p}{\partial z}+\mu\nabla^2 w+\rho\beta\vec{g}_z(T-T_{ref})+\frac{(1-\gamma)^2}{(\gamma^3+\varepsilon)}A_{mush}w \tag{4}$$

Energy Equation [7,17,19]:

$$\frac{\partial}{\partial t}(\rho H)+\frac{\partial}{\partial x}(\rho u H)+\frac{\partial}{\partial y}(\rho v H)+\frac{\partial}{\partial z}(\rho w H)=\frac{\partial}{\partial x}\left(k\frac{\partial T}{\partial x}\right)+\frac{\partial}{\partial y}\left(k\frac{\partial T}{\partial y}\right)+\frac{\partial}{\partial z}\left(k\frac{\partial T}{\partial z}\right) \tag{5}$$

When creating numerical models to simulate the melting process of PCMs, several assumptions are typically considered. These assumptions are derived from established practices and prior research within the field [7,17].

- The thermo-physical characteristics of PCMs are assumed to be invariant.
- The liquid PCM flow is modeled as three-dimensional, transient, laminar, incompressible, and Newtonian.
- Volume changes due to phase transitions are disregarded.
- The Boussinesq approximation is applied, considering density variations only in relation to temperature.

Total energy storage in the context of Phase Change Materials (PCM) refers to the cumulative thermal energy that the material can absorb during the phase transition from solid to liquid. This energy storage capacity is crucial for effective thermal management in various applications, including building materials, thermal batteries, and heat exchangers. The total energy storage can be expressed using the enthalpy equation, which accounts for both sensible and latent heat. The equation is formulated as follows [7,17]:

$$H=h+\int_{T_{ref}}^{T}C_p dT+\gamma L_h \tag{6}$$

where, H is the total enthalpy (J/kg), h is the reference sensible enthalpy (J/kg), Cp is the specific heat capacity (J/kg·K), T is the temperature (K), T_{ref} is the reference temperature (K), γ is the liquid fraction ($0 \le \gamma \le 1$), and $L_h$is the latent heat of fusion (J/kg).

The liquid fraction is defined using the following expression [7,17]:

$$\gamma=\begin{cases}0, & T<T_s\\ \dfrac{T-T_s}{T_l-T_s}, & T_s<T<T_l\\ 1, & T>T_l\end{cases} \tag{7}$$

Initial and Boundary Conditions:

Case 1:

$$\begin{aligned}&\text{Allwalls}: u=v=w=0\ \text{m/s}\\ &\text{Foroutersurface}: T_\infty = 40^\circ\text{C} = 313.15\ \text{K},\ h_{\text{nat\_conv}} = 2.88\ \text{W/m}^2\text{K}\\ &\text{Forinnersurface}: T_{\text{skin}} = 34.5^\circ\text{C} = 307.65\ \text{K},\ h_{\text{nat\_conv}} = 2.88\ \text{W/m}^2\text{K}\end{aligned} \tag{8}$$

Case 2:

$$\begin{aligned}&\text{Allwalls}: u=v=w=0\text{m/s}\\ &\text{Foroutersurface}: T_\infty = 50^\circ\text{C} = 323.15\ \text{K},\ h_{\text{natrual}} = 2.88\ \text{W/m}^2\text{K}\\ &\text{Forinnersurface}: T_{\text{skin}} = 34.5^\circ\text{C} = 307.65\ \text{K},\ h_{\text{nat\_conv}} = 2.88\ \text{W/m}^2\text{K}\end{aligned} \tag{9}$$

The surface and skin boundary condition can be represented as [20]

$$q_o = h(T-T_\infty \tag{10}$$

4. Numerical methods

This study utilizes Fluent software version 2024R1 to solve the governing equations (Eqs. 1 to 5) and boundary conditions (Eqs. 8 and 9). To account for buoyancy effects, the Boussinesq approximation is applied to the density in the material properties section. The analysis incorporates transient effects and gravitational acceleration. For transient discretization, a second-order implicit scheme is used, while the SIMPLE algorithm facilitates the coupling of pressure and velocity. Pressure corrections are handled with the PRESTO algorithm, and the momentum and energy equations are spatially discretized using the second-order upwind scheme. A least-squares cell-based gradient method is also employed for calculations. Residual tolerances for all variables are set to 10^{-6}, and a time step of 1 s is applied, with 40 iterations per time step to meet the convergence criteria ($\le 10^{-6}$).

The simulation workflow in Ansys Workbench for fluid flow analysis follows a structured approach. It begins with defining the physical domain using the New Design Modeler, followed by mesh generation to discretize the geometry. The simulation setup involves specifying transient and gravity effects, alongside selecting appropriate models such as energy, viscous laminar flow, and solidification/melting. Material properties and boundary conditions are then assigned to ensure accurate representation of real-world conditions. The solution phase includes defining methods, controls, and monitoring parameters before executing the calculations. Finally, post-processing is performed to analyze results, visualize data, and extract meaningful insights from the simulation. The numerical procedure is illustrated in the flow chart in Fig. 2.

5. Validation

To evaluate the reliability of the present numerical model, validation was conducted using both experimental and numerical reference studies.

First, the model was validated against the experimental data of Kamkari et al. [21], who studied the melting behavior of PCM under natural convection in a rectangular enclosure. The trends of liquid fraction evolution over time observed in our study closely matched their results, confirming the model's ability to accurately capture phase change behavior and heat transfer mechanisms under natural convection.

Additionally, the present study was validated against the numerical work of Nagaraju et al. [7], who analyzed a thermal energy storage (TES) system for helmet cooling using RT-27 and Capric Acid under

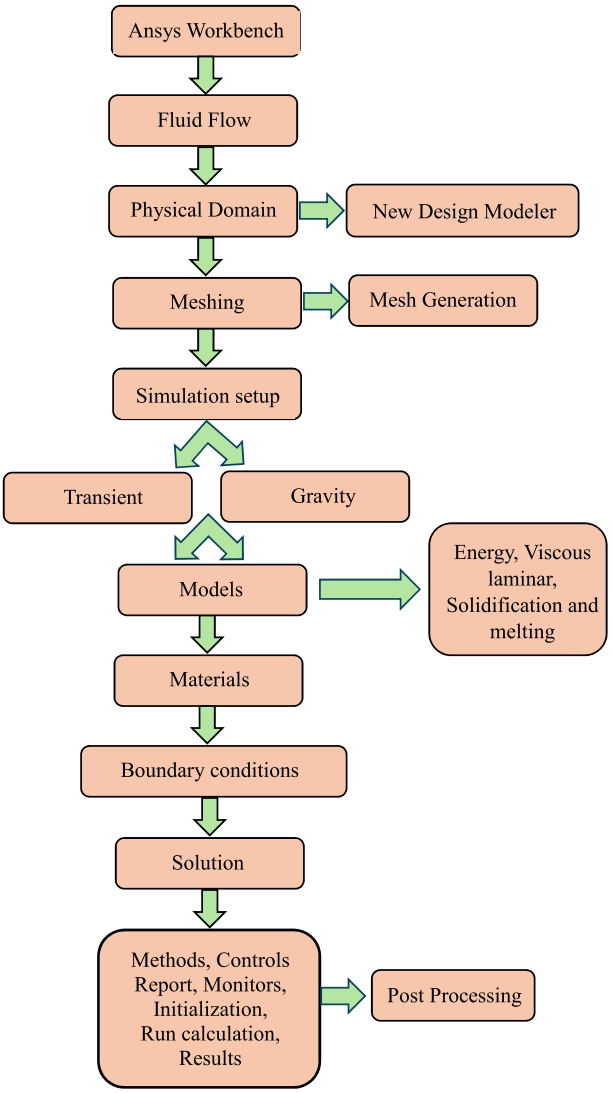

Fig. 2. Flow chart of the numerical procedure in Fluent.

natural convection. The comparison focused on the liquid fraction progression and average temperature for the vertical orientation and upper tube configuration for both PCMs. The results demonstrated consistent melting times and temperature profiles, especially the faster melting behavior of RT-27 and the extended phase transition of Capric Acid, affirming the accuracy of our simulation approach in modeling multi-PCM systems in wearable applications. Fig. 3 illustrates the variation of liquid fraction and average temperature over time, highlighting the strong agreement with the referenced studies.

6. Mesh independent test

A Mesh independence analysis was performed to identify the optimal mesh that strikes a balance between computational efficiency and result precision. Six different mesh configurations, incorporating wall refinement, were tested to assess the sensitivity of the mesh by analyzing the influence of element size on computational outcomes. The study examined the variation of average temperature (T) and liquid fraction (LF) over time for each mesh. Fig. 4 presents the 3D mesh of the model and the variations of temperature (T) and liquid fraction (LF) for different numbers of elements. The results indicate that Mesh 4, 5, and 6 yield consistent outcomes. Mesh 4 was chosen for subsequent analyses as it offers an optimal trade-off between computational performance and numerical accuracy.

7. Findings and discussion

This study evaluates the thermal performance of a cap integrated with two PCMs, RT-27 and Capric Acid, designed to protect the human head from extreme heat. The cap is constructed with three layers: an upper and a lower layer made of a wool and cotton mixture, and a middle layer housing the PCMs. This innovative design ensures both immediate and sustained protection from heat by leveraging the complementary thermal properties of the PCMs.

7.1. Case 1

Fig. 5a–5c demonstrates the changes in LF and T over time at a constant temperature of 40 °C. RT-27, with a melting point of 27 °C, begins melting quickly and reaches full liquefaction by 155 min. Its rapid phase transition makes it highly effective in absorbing heat during the initial exposure period, providing immediate cooling and stabilizing the head's temperature. This characteristic is especially beneficial for short-term applications where quick relief from heat is critical, such as during the onset of intense physical activity. In contrast, Capric Acid, which has a higher melting point of around 31–32 °C, melts more gradually, taking up to 230 min for complete melting. Its slower melting rate allows it to provide prolonged thermal protection after RT-27 has fully transitioned to the liquid phase. This extended melting period ensures sustained cooling, making it ideal for long-term activities requiring continuous heat mitigation, such as extended work shifts or prolonged outdoor exposure. RT-27 offers rapid thermal relief during the initial stages of heat exposure, while Capric Acid ensures a steady and extended cooling effect as the exposure duration increases. These PCMs enable the cap to maintain an optimal thermal environment for the head over several hours. The results, illustrated in Fig. 5, detail the liquid fraction and temperature evolution for each PCM at specific time intervals (1, 60, 155, and 230 min). Initially, both PCMs remain in their solid state, effectively insulating the head from external heat, maintaining a uniform temperature closer to their solidus point (24 °C). The outer layers of wool and cotton provide insulation, preventing rapid heat transfer into the inner layers and maintaining a low-temperature gradient. This ensures that the head remains insulated from external heat during the early stages of exposure. RT-27 demonstrates a rapid transition to the liquid phase within the first 60 min, with significant heat absorption occurring during this period. Capric Acid, however, retains much of its solid state during this time and gradually melts, achieving full liquefaction by 230 min. This staggered phase change ensures continuous cooling, with no significant lapse in thermal protection throughout the period. By 155 min, RT-27 is fully liquefied, marking the end of its heat-absorbing capacity.

60 to 90 Min: At this stage, RT-27 has undergone approximately half of its phase transition, stabilizing the temperature within its region at 25.7 °C. The insulating wool and cotton layers continue to impede heat transfer, causing the outer layer temperature to reach 27.7 °C by 90 min. Meanwhile, Capric Acid begins to melt more significantly, effectively absorbing heat. This process helps maintain a lower temperature in the middle layer, where it stabilizes at ~26.78 °C, and in the inner layer at ~27.24 °C. By the 90-minute mark, the temperature of Capric Acid gradually rises, ranging from ~27.97 °C to 29.9 °C across all layers.

155 to 230 Min: RT-27 fully transitions to a liquid state and depletes its latent heat, resulting in a gradual rise in temperature. By 155 min, the cap's inner layer reaches its maximum temperature of 34.12 °C. In contrast, Capric Acid undergoes a prolonged melting process, stabilizing its temperature near its melting point (~31–32 °C). This property allows Capric Acid to extend thermal regulation up to 230 min, maintaining lower inner-layer temperatures, while the upper surface temperature peaks at 36.77 °C.

In summary, RT-27 undergoes rapid melting, making it ideal for short-term cooling, while Capric Acid melts more gradually, offering sustained thermal regulation over an extended period. The latent heat of

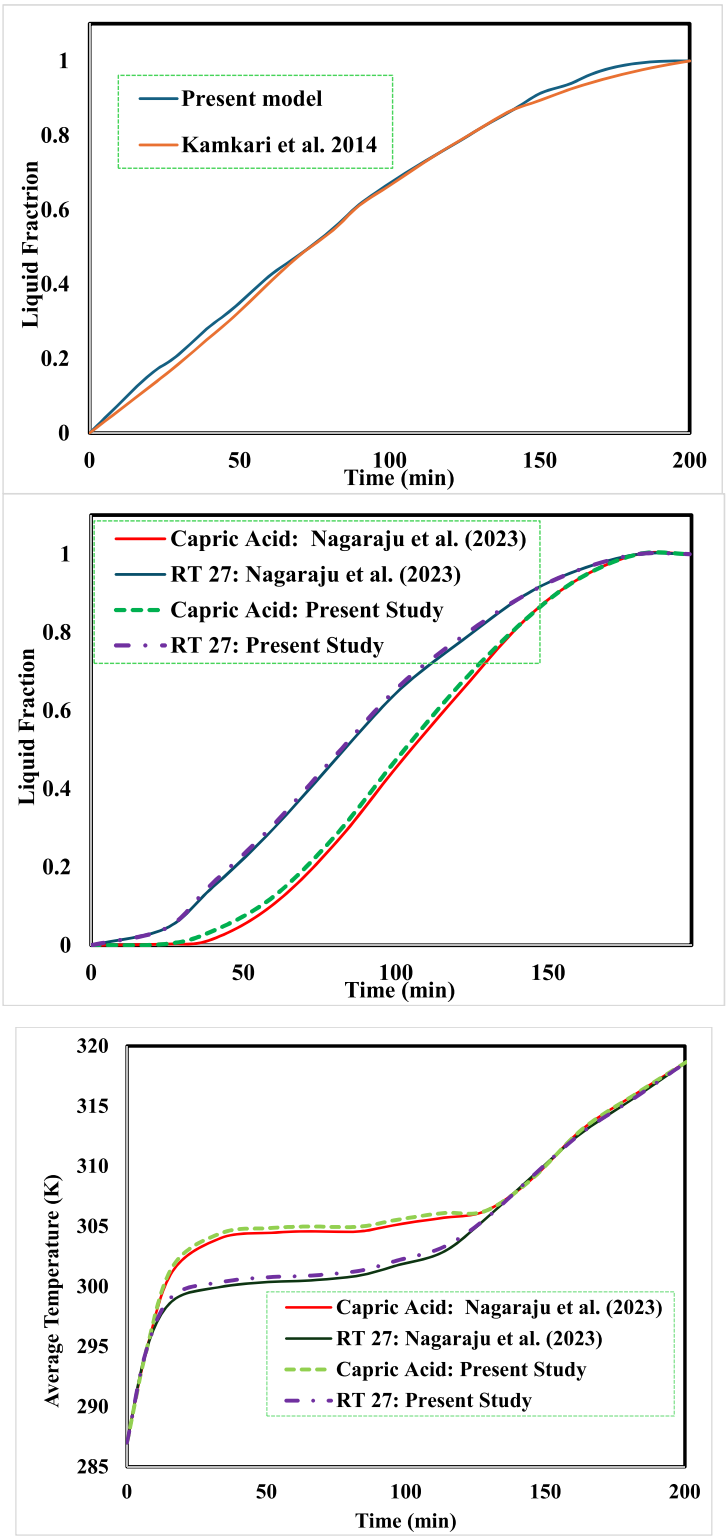

Fig. 3. Variation of liquid fraction, and average temperature with time (min).

fusion of each PCM plays a crucial role in delaying temperature rise. RT-27 absorbs heat efficiently in the early phase, while Capric Acid provides a longer duration of thermal protection, ensuring a prolonged cooling effect depending on the application. The wool-cotton outer layers act as a thermal barrier, slowing heat transfer and maintaining a stable temperature gradient. This insulation effect enhances the cooling efficiency of both PCMs by reducing direct heat exposure.

7.2. Case 2

Fig. 6a–6c demonstrates the changes in LF and Temperature over time at a constant temperature of 50 °C, highlighting the distinct thermal behaviors of PCM 1 (RT-27) and PCM 2 (Capric Acid). PCM 1 exhibits a faster melting rate, with significant liquid fraction development and half-complete melting achieved by 60 min. Complete melting occurs in 108 min, demonstrating its ability to absorb and dissipate heat

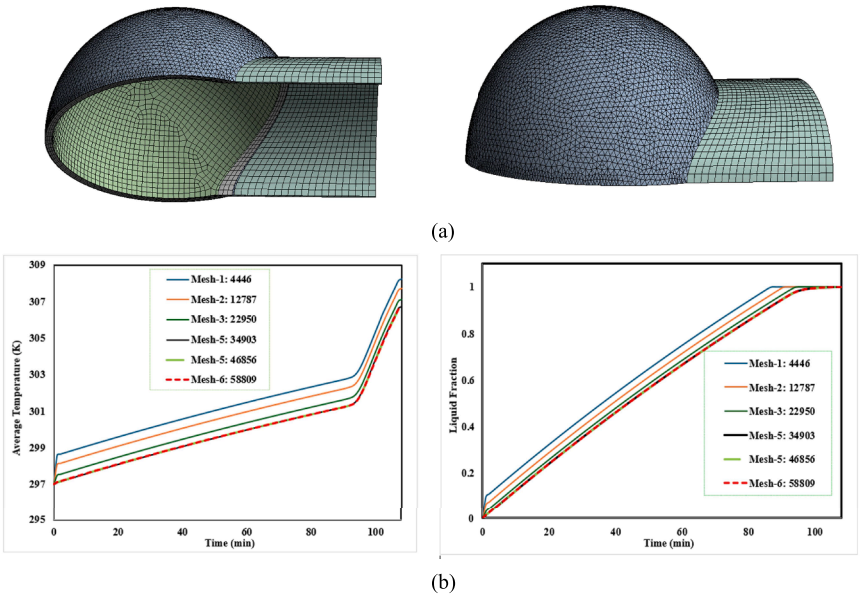

Fig. 4. (a) 3D finite volume mesh of the model and (b) variation of average temperature and liquid fraction with time (min) for various mesh sizes.

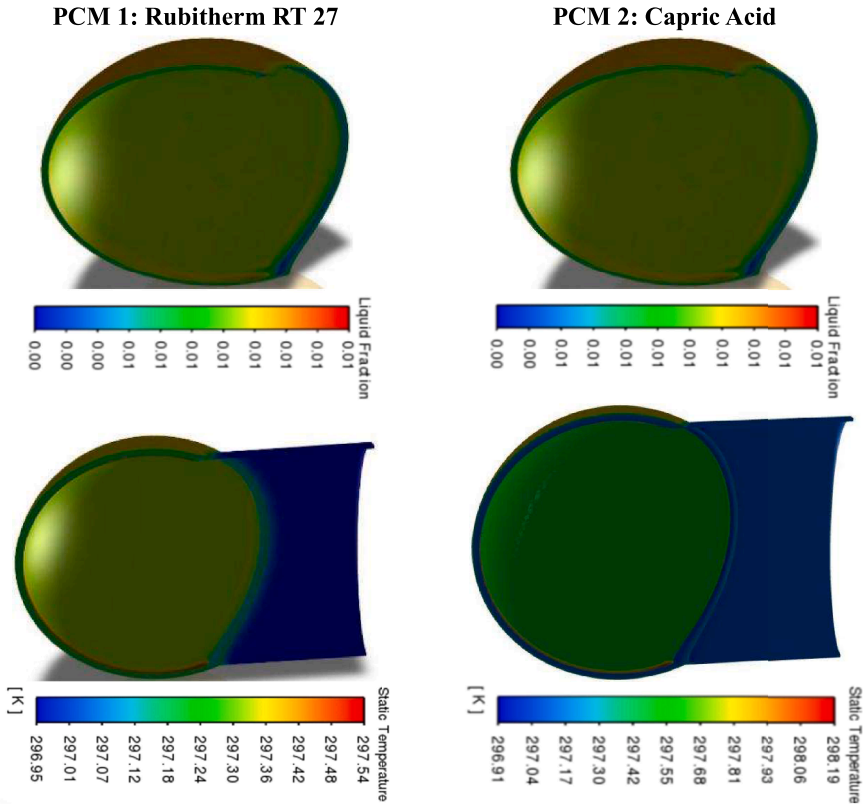

Fig. 5a. Liquid fraction (LF) and Temperature after 1 min when $T = 40$ °C.

effectively in the initial stages of exposure. This rapid thermal response makes PCM 1 ideal for applications requiring immediate cooling, such as for athletes or laborers exposed to sudden heat surges. In contrast, PCM 2 demonstrates a slower melting behavior, with noticeable melting beginning at 60 min. Complete melting occurs in 133 min, indicating its capacity for prolonged heat absorption and thermal regulation. This characteristic makes PCM 2 suitable for extended exposure to high temperatures, such as for outdoor workers or individuals in hot climates.

Initial Phase (1 min): At the 1-minute mark, both PCMs effectively regulate the inner layer temperature near room temperature. RT-27 stabilizes at approximately 24 °C, while Capric Acid demonstrates slightly better thermal regulation at comparable levels. The outer layer temperature shows a slight increase but remains below 25 °C, highlighting the efficient initial heat absorption of the PCM.

Prolonged Exposure (60–90 min): At 60 min, RT-27 demonstrates significant heat transfer, with the inner layer reaching approximately 27.1 °C and the middle layer exceeding 26.7 °C. In contrast, Capric Acid provides better thermal stability, maintaining the inner layer at about

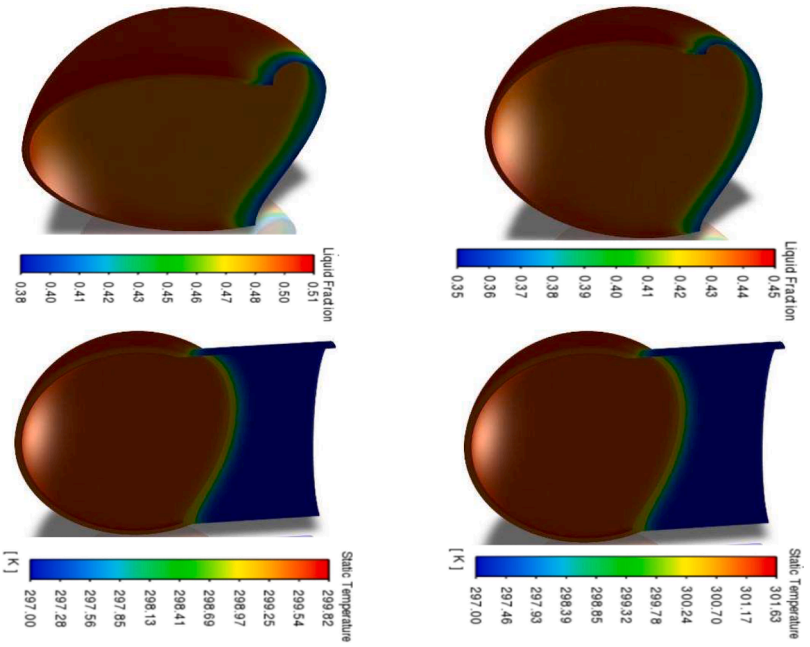

Fig. 5b. Liquid fraction (LF) and Temperature after 60 min when $T = 40$ °C.

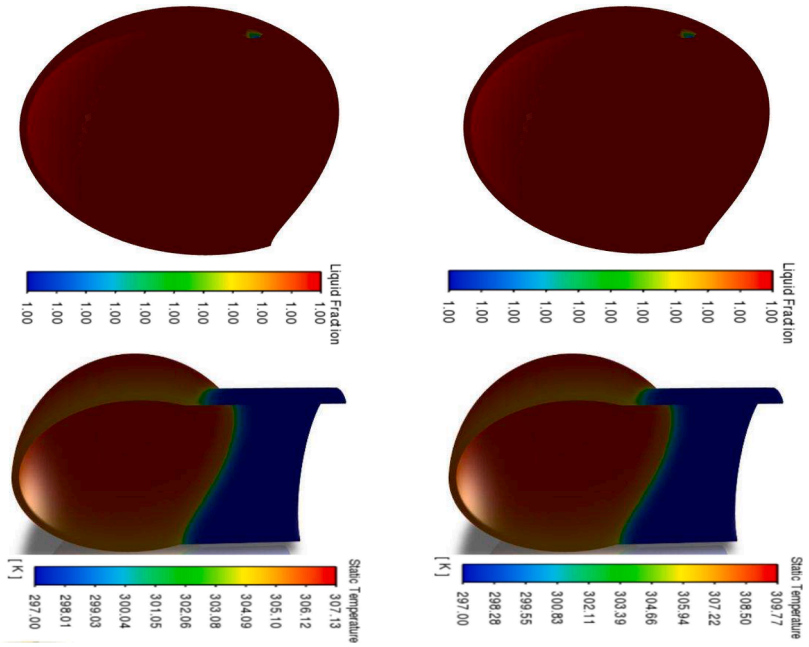

Fig. 5c. Liquid fraction (LF) and Temperature after 155 mins (RT-27) and 230 mins (Capric Acid) when $T = 40$ °C.

28.98 °C and the middle layer at 28.36 °C. By 90 min, RT-27 exhibits a temperature range of 27.82 °C to 29.5 °C across all layers, while Capric Acid continues to offer enhanced thermal protection, keeping the inner layer below 30.57 °C.

Critical Time Points (108–133 min): The RT-27 depletes its latent heat over a duration of 108 min, maintaining a lower inner layer temperature throughout this period. The cap reaches its maximum temperature of 36.96 °C at the top. In contrast, Capric Acid extends the protection for up to 133 min, maintaining lower inner-layer temperatures for a longer period. During this time, the temperature of the upper surface of the cap reaches 38.83 °C.

The innovative design of the cap leverages the thermal properties of RT-27 and Capric Acid, combined with the insulation benefits of wool and cotton layers, to provide effective and sustained protection against heat. RT-27, with its lower melting point, acts as the primary heat absorber during initial exposure to high temperatures, delivering rapid cooling and maintaining a stable temperature in the middle layer. Capric Acid, with its higher latent heat capacity, ensures prolonged thermal regulation by continuing to absorb heat even after RT-27 has fully melted, making it ideal for extended periods of exposure. The wool and cotton layers, placed in the upper and lower sections of the cap, enhance their performance by reducing the rate of heat transfer from the environment to the PCMs. This insulation not only slows the melting process of the PCMs but also prevents rapid temperature rise in the inner layers, ensuring consistent cooling.

The breathable and soft texture of wool and cotton adds comfort,

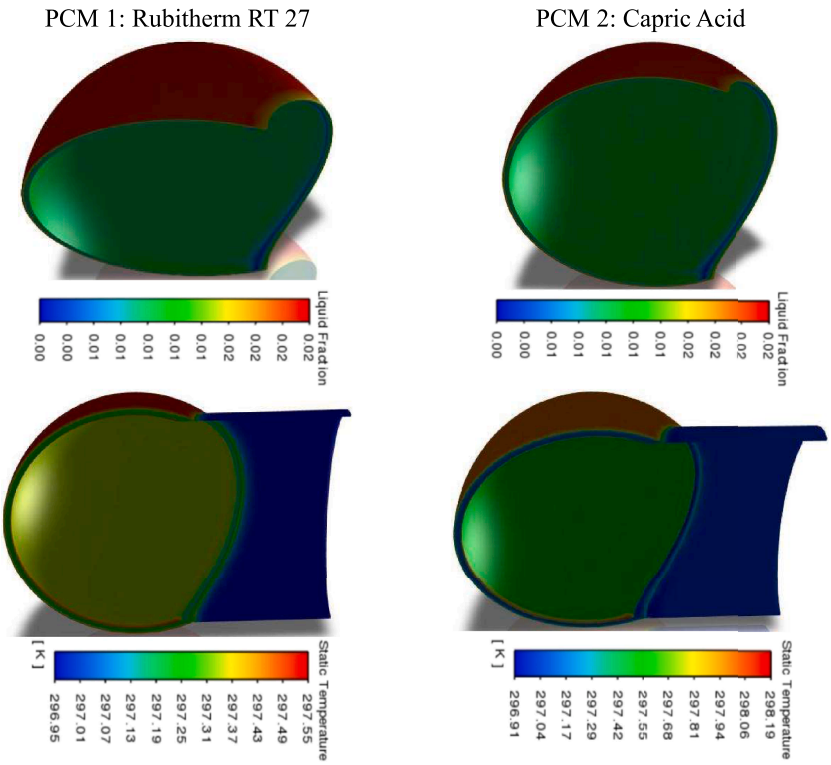

Fig. 6a. Liquid fraction (LF) and Temperature after 1 min when $T = 50$ °C.

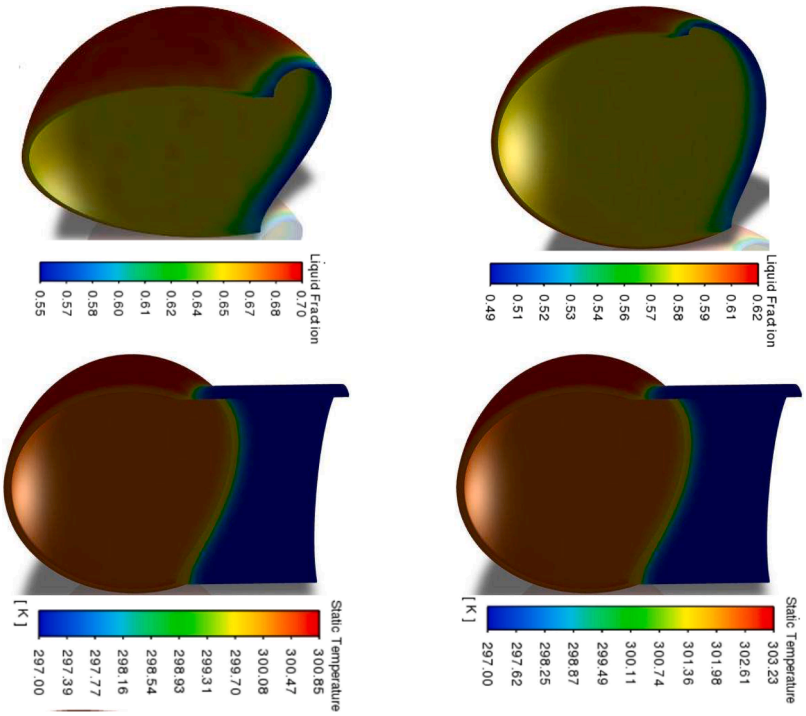

Fig. 6b. Liquid fraction (LF) and Temperature after 60 min when $T = 50$ °C.

making the cap suitable for prolonged use in scenarios such as athletic performance, industrial labor, and outdoor activities in high-temperature environments. Athletes benefit from the immediate cooling provided by RT-27 during intense activity and the sustained cooling by Capric Acid during rest periods. Laborers and outdoor workers experience reduced heat stress and enhanced safety, while individuals in extreme climates, such as deserts, find the cap effective for maintaining head temperature and comfort during prolonged exposure.

The cap's lightweight design further enhances user experience, ensuring practicality for extended wear. Numerical analysis validates the cap's ability to mitigate heat-related risks by maintaining a favorable temperature gradient across its layers. RT-27 excels in scenarios

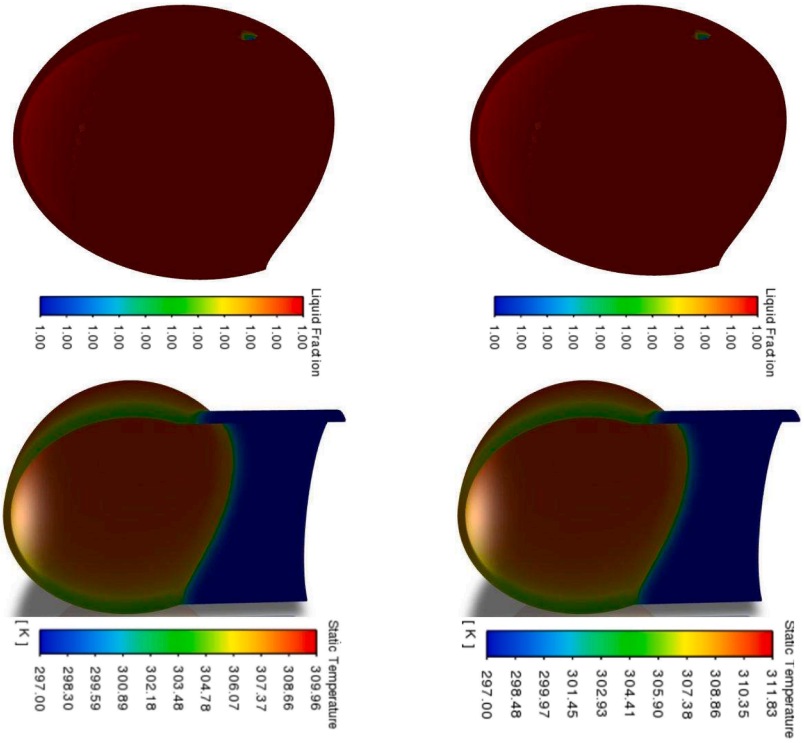

Fig. 6c. Liquid fraction (LF) and Temperature after 108 mins (RT-27) and 133 mins (Capric Acid) when $T = 50$ °C.

requiring rapid protection during brief, high-intensity heat exposure, while Capric Acid offers superior thermal stability and extended protection, particularly in extreme heat conditions. The integration of these PCMs, combined with effective insulation, ensures consistent thermal regulation and safety in diverse applications.

To validate the model and position the findings in a broader context, this study was compared against relevant literature. For instance, Nagaraju et al. [7] reported that RT-27 melted in 150 min and Capric Acid in 175 min under natural convection in helmet-based systems. In our study, RT-27 completed melting in 155 min, and Capric Acid in 230 min at 40 °C—indicating enhanced cooling duration due to the added textile insulation and layered structure of the cap.

Similarly, Ghani et al. [10] demonstrated that PCM-enhanced helmets could reduce head temperatures by ~10 °C below ambient. Our results showed a temperature reduction of 6–14 °C, depending on the PCM and ambient temperature (40 °C or 50 °C), confirming strong thermal performance. Tan and Fok [8] achieved ~2 h of comfort cooling using PCM pouches, while our RT-27 layer alone provided 155 min of

Table 3
Comparison of previous helmet cooling studies and present work.

Study	PCM Used	Melting Temp (°C)	Cooling Duration	Max Temp Reduction	Configuration	Key Findings	Comparison to Present Study
Omara et al. [6]	Multiple PCMs	~25–35	~2 h	~5 °C	Helmet with PCM pads	PCMs can maintain comfort temp; issues with condensation	Similar concept; cap design avoids condensation via textile insulation
Nagaraju et al.[7]	RT-27, Capric Acid	27, 32	RT-27:150 min Capric Acid: 175 min	~6 °C	Helmet with TES system	RT-27 melts faster; Capric Acid provides prolonged cooling	Our results: RT-27 (155 min), Capric Acid (230 min); longer cooling due to fabric insulation
Tan & Fok[8]	Not specified	~28	~2 h	~4–5 °C	Helmet pouch	Heat transfer via conduction without power	Our model Also passive but offers longer cooling due to dual PCM
Reddy & Reddy[9]	S25, S27 (Salt hydrates)	36, 34	Up to 4.99 h	Not specified	Motorcycle helmet	Higher melting temp gives longer duration	Our lower melting PCMs are ideal for faster cooling, less suited to high-intensity radiation
Ghani et al. [10]	PCM pad + forced convection	24	>2 h	Up to 10 °C	Industrial helmet with forced air	Forced convection improves cooling efficiency	Our design is passive, but shows ~7–10 °C lower than ambient at 40–50 °C
Ali et al.[11]	Nano-enhanced paraffin	35	>4 h	Significant	Composite in safety helmet	Improved thermal conductivity and duration	We used standard PCMs but achieved similar duration using textile insulation
Venugopal et al.[12]	NPG + CuO/ Al_2O_3 /TiO_2	40–45	Not specified	20 % temp reduction	Enhanced nano-PCM	Best conductivity with CuO, reduced helmet temp	Our solution is simpler and cost-effective but slightly less effective in extreme heat
Sinnappoo et al.[13]	Sustainable paraffins	~34	~2 h	3.8 °C	Textile liner in helmet	Practical and eco-friendly cooling	Our cap uses traditional PCMs but outperforms in duration
Al-Rjoub et al.[14]	PCM + helical exchanger	~28–30	100 min	~6 °C	Portable cooling system	Effective 40 W load Management	Our cap manages ambient heat passively; more wearable/ flexible

relief, and Capric Acid extended protection up to 230 min.

These comparisons reinforce the reliability of the simulation model and show that our PCM-cap design delivers comparable or superior performance to traditional helmet systems, with added benefits in flexibility, comfort, and wearability. Table 3 presents a side-by-side comparison of key studies on helmet cooling with PCMs and highlights the improved performance of the current study.

8. Quantitative analysis

This study evaluates the thermal performance of a cap integrated with two distinct phase change materials (PCMs), RT-27 and Capric Acid, under two ambient temperatures (40 °C and 50 °C). The cap, which includes three layers with wool-cotton insulation, was analyzed in terms of liquid fraction (LF), temperature (T), and total energy absorption (E) over time. The numerical results offer valuable insights into the phase change behavior and thermal management efficiency of each

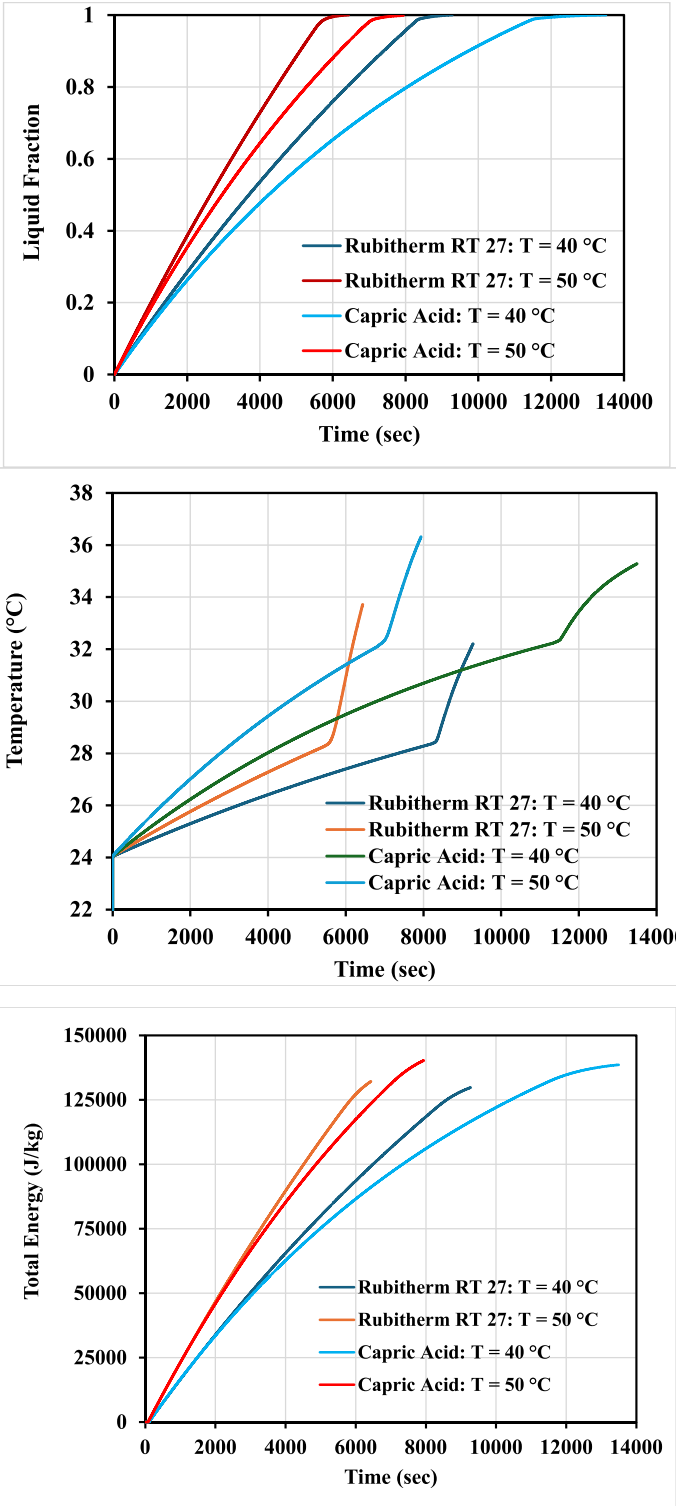

Fig. 7. Variation of Liquid fraction, temperature and total energy with time (*sec*).

PCM, helping us understand how these materials react to different environmental conditions and their potential application in wearable thermal regulation. Fig. 7 shows the changes in LF, T, and total E over time.

8.1. Liquid fraction (LF) and phase change dynamics

At 40 °C, RT-27 undergoes a rapid phase change, reaching 90 % liquid fraction in 7396 s (123.3 min), and completes its melting at 92,710 s (155 min). This quick transition can be attributed to RT-27′s relatively low latent heat of fusion and its low melting point (27 °C), which allows it to absorb heat quickly. The steep phase change curve indicates a highly efficient heat absorption process in the early stages, which provides rapid thermal relief during the initial period of exposure.

In contrast, Capric Acid exhibits a slower phase change. It reaches 75 % liquid fraction at 7396 s (123.3 min) and completes melting at 13,500 s (225 min). This slower rate is due to Capric Acid's higher latent heat capacity and its higher melting point (~31–32 °C). As a result, Capric Acid absorbs heat more gradually, extending the cooling effect and providing sustained thermal regulation over a longer period. This slower melting rate makes Capric Acid a better choice for applications requiring prolonged thermal protection.

At 50 °C, both PCMs demonstrate a faster phase change, but the differences in their thermal behaviors remain clear. RT-27 reaches 100 % liquid fraction in just 6480 s (108 min), reflecting the material's rapid absorption of heat. The steep phase change curve seen at 50 °C contrasts with the more gradual behavior of Capric Acid, which reaches 93 % liquid fraction at 6480 s (108 min) and completes melting by 7980 s (133 min). This highlights Capric Acid's superior latent heat capacity and extended cooling period, even at higher ambient temperatures.

8.2. Temperature response and thermal regulation

At 40 °C, the average temperature of the cap with RT-27 rises to 28.5 °C over 8324 s (138.73 min). As RT-27 melts, its temperature increases more rapidly, reaching 32.5 °C upon complete phase transition. This rapid increase in temperature occurs once the PCM has finished melting and is no longer absorbing heat. During melting, the PCM maintains a near-constant temperature, providing effective thermal buffering. However, once liquefied, RT-27 can no longer absorb latent heat, and the temperature increases sharply, indicating the end of its cooling capacity.

In comparison, Capric Acid maintains a more stable temperature throughout its melting process. At 40 °C, the inner temperature of the cap stays below 32.34 °C for 11,460 s (191 min), providing better thermal regulation and comfort. Once Capric Acid completes its phase change, the temperature stabilizes at around 35.26 °C, which remains within a comfortable range. This extended period of temperature stability is a direct result of the material's slower melting process and higher latent heat capacity, which allows it to absorb and release heat gradually over a longer period.

At 50 °C, RT-27 causes the inner layer temperature to rise to 28.4 °C over 5570 s (92.83 min), with a rapid temperature increase to 34 °C as melting completes. This behavior underscores the rapid absorption and release of heat by RT-27, which is well-suited for short-term cooling needs. On the other hand, Capric Acid maintains the inner layer temperature below 32.5 °C for 7030 s (117.2 min), demonstrating superior thermal regulation, even under higher ambient temperatures. Once Capric Acid has fully melted, the temperature remains below 36 °C, showcasing its ability to provide prolonged cooling and protection in more extreme conditions.

8.3. Total energy absorption and thermal buffering capacity

The total energy absorbed by each PCM also reflects their differences in latent heat and phase change behavior. At 40 °C, PCM 1 absorbs approximately 130 kJ/kg of energy during its phase change before plateauing, indicating the completion of its heat absorption capacity. In contrast, Capric Acid absorbs 139 kJ/kg, continuing to store energy beyond its phase change and thus offering extended thermal protection. This extended energy storage allows Capric Acid to maintain a stable temperature over a longer period, which is crucial for applications requiring sustained thermal regulation.

At 50 °C, RT-27 absorbs 131 kJ/kg during its phase change, with energy absorption again plateauing once melting is complete. Capric Acid, however, absorbs 140 kJ/kg, continuing to store energy, further enhancing its ability to regulate temperature even under more extreme conditions. The continued energy absorption of Capric Acid at higher temperatures highlights its superior thermal buffering capacity, which makes it more effective for long-duration thermal protection in hot environments.

The study's results highlight several key thermal mechanisms at play:

Both PCMs rely on latent heat absorption during their phase transitions, stabilizing the temperature during melting and providing significant thermal buffering. RT-27′s rapid phase change is driven by its lower latent heat, making it more suitable for short-term cooling, while Capric Acid's higher latent heat capacity ensures extended thermal regulation, making it ideal for prolonged cooling applications. The wool-cotton insulation slows the rate of heat transfer into the cap, prolonging the phase change process and maintaining a stable temperature gradient. These insulating layers act as an additional buffer, preventing rapid temperature rise and further enhancing the cooling efficiency of both PCMs. The results demonstrate that while both PCMs perform well at 40 °C, Capric Acid's advantages become more apparent at 50 °C, where it provides superior long-duration thermal protection.

9. Conclusions

The present study focused on the numerical investigation of a wearable cap designed for thermal protection in extreme heat, using two Phase Change Materials (PCMs): Rubitherm RT-27 and Capric Acid. A multi-layer cap structure was modeled, incorporating PCM and insulation layers, and simulations were performed under natural convection to assess temperature regulation, liquid fraction evolution, and energy storage. Validation and mesh independence studies ensured model reliability. Based on the analysis, the following conclusions are drawn:

- The cap structure with dual PCMs effectively maintained inner-layer temperatures 6–14 °C below ambient across varying conditions (40 °C and 50 °C), offering reliable passive cooling performance.
- RT-27, with a lower melting point (27 °C), melted rapidly within 155 min at 40 °C and 108 min at 50 °C, making it ideal for short-term, immediate thermal relief.
- Capric Acid, with a higher latent heat and melting point (~32 °C), demonstrated prolonged cooling—230 min at 40 °C and 133 min at 50 °C, confirming its suitability for long-duration applications.
- The staggered melting behavior of the 2 p.m. provided both initial and sustained cooling, eliminating thermal performance gaps and extending effective thermal regulation time.
- The wool-cotton insulation layers enhanced the performance by delaying heat penetration and prolonging PCM phase transitions, thereby improving both comfort and energy storage efficiency.
- A mesh independence test confirmed the optimal mesh configuration, ensuring computational accuracy and efficiency. The numerical model was validated against previous experimental and computational studies, showing strong agreement.
- In comparison to prior PCM-helmet designs, the cap achieved comparable or better cooling durations, with added advantages of lightweight construction, textile flexibility, and enhanced wearability.

- The use of passive PCM cooling, without active mechanisms or external power sources, makes the design feasible for athletes, industrial workers, military personnel, and individuals in hot climates.

This study demonstrates the viability of PCM-integrated textile caps as a practical, wearable solution for mitigating heat stress. The proposed design bridges the gap between comfort and performance in wearable thermal protection and provides a foundation for further development of passive cooling apparel in extreme environments.

10. Limitations and future directions

This study, while demonstrating the effectiveness of PCM-integrated caps for thermal regulation, has several limitations. The findings are based on numerical simulations, requiring experimental validation for real-world applicability. The study assumes constant PCM properties and simplified boundary conditions, excluding factors like wind, humidity, and solar radiation. Additionally, only 2 p.m. (RT-27 and Capric Acid) were analyzed, and user comfort aspects were not assessed.

Future research should focus on experimental testing under dynamic environmental conditions. Optimization of PCM selection, including hybrid or nano-enhanced PCMs, could improve thermal performance. Investigating ergonomic design, breathability, and weight distribution will enhance wearability. Integrating active cooling mechanisms with PCMs could extend cooling duration. Application-specific modifications for industrial workers, athletes, and military personnel should also be explored. Addressing these aspects will advance PCM-based wearable cooling solutions, making them more effective and adaptable for extreme heat conditions.

Financial support and sponsorship

None.

Ethical approval and consent to participate

Not applicable.

AI declaration

The authors used AI-assisted technology (ChatGPT-3.5) for language editing and grammar checking.

CRediT authorship contribution statement

Mohammad Junaid: Writing – review & editing, Writing – original draft, Visualization, Validation, Software, Resources, Methodology, Investigation, Formal analysis, Data curation. **Goutam Saha:** Writing – review & editing, Writing – original draft, Visualization, Supervision, Software, Methodology, Investigation, Formal analysis, Conceptualization. **Pabel Shahrear:** Writing – review & editing, Writing – original draft. **Suvash C. Saha:** Writing – review & editing, Writing – original draft.

Declaration of competing interest

The authors declare that they have no known competing financial interests or personal relationships that could have appeared to influence the work reported in this paper.

Data availability

No data was used for the research described in the article.

References

[1] L. Zhao, M. Oppenheimer, Q. Zhu, J.W. Baldwin, K.L. Ebi, E. Bou-Zeid, K. Guan, X. Liu, Interactions between urban heat islands and heat waves, Environ. Res. Lett. 13 (3) (2018) 034003.
[2] S.E. Kalnæs, B.P. Jelle, Phase change materials and products for building applications: a state-of-the-art review and future research opportunities, Energy Build. 94 (2015) 150–176.
[3] F. Wang, D. Pang, X. Liu, M. Liu, W. Du, Y. Zhang, X. Cheng, Progress in application of phase-change materials to cooling clothing, J. Energy Storage 60 (2023) 106606, https://doi.org/10.1016/j.est.2023.106606.
[4] S. Mondal, Phase change materials for smart textiles – An overview, Appl. Therm. Eng. 28 (11) (2008) 1536–1550, https://doi.org/10.1016/j.applthermaleng.2007.08.009.
[5] X. Wang, W. Zhao, J. Pollard, S.S. Xu, Experimental study on the thermal protection enhancement of novel phase change material integrated structural firefighting gloves under high-heat exposures, Case Studies Thermal Eng. 56 (2024) 104286, https://doi.org/10.1016/j.csite.2024.104286.
[6] A.A.M. Omara, A.A.M. Mohammedali, R. Dhivagar, Helmets cooling with phase change materials: a systematic review, J. Energy Storage 72 (2023) 108555, https://doi.org/10.1016/j.est.2023.108555. -.
[7] D. Nagaraju, B.V.S.R.N. Santhosi, A.R. Mohammad, J. Syed, N.K. Kolla, Numerical investigation of sustainable thermal energy storage (TES) system for personal helmet cooling, Int. J. Thermofluids 20 (2023) 100481, https://doi.org/10.1016/j.ijft.2023.100481.
[8] F.L. Tan, S.C. Fok, Cooling of helmet with phase change material, Appl. Therm. Eng. 26 (17) (2006) 2067–2072, https://doi.org/10.1016/j.applthermaleng.2006.04.022.
[9] M.M. Reddy, A.H.V. Reddy, Conserving impact on two wheeler helmet with phase change substance, Int. J. Innov. Technol. 8 (2) (2020) 126–131. Link, https://ijitech.org/uploads/142356IJIT17682-28.pdf.
[10] S. Ghani, E.M.A.A. ElBialy, F. Bakochristou, S.M.A. Gamaledin, M.M. Rashwan, The effect of forced convection and PCM on helmets' thermal performance in hot and arid environments, Appl. Therm. Eng. 111 (2017) 624–637, https://doi.org/10.1016/j.applthermaleng.2016.09.142.
[11] M.A. Ali, Fayaz, R.F. Viegas, M.B. Shyam Kumar, R.K. Kannapiran, M. Feroskhan, Enhancement of heat transfer in paraffin wax PCM using nano graphene composite for industrial helmets, J. Energy Storage 26 (2019) 100982, https://doi.org/10.1016/j.est.2019.100982.
[12] A. Venugopal, K.K. Anzil, B.G. Thomas, J.T. Varghese, Nano-enhanced phase change material for thermal comfort at skull and environment interface in riding helmets: an experimental investigation, J. Energy Storage 50 (2022) 104332, https://doi.org/10.1016/j.est.2022.104332.
[13] K. Sinnappoo, R. Nayak, L. Thompson, R. Padhye, Application of sustainable phase change materials in motorcycle helmet for heat-stress reduction, J. Text. Inst. 111 (11) (2020) 1547–1555, https://doi.org/10.1080/00405000.2020.1715606.
[14] M. Al-Rjoub, M.J. Kazmierczak, A. Bhattacharya, S. Rakkimuthu, S. Ramadurai, J. P. Stuckey, R.K. Banerjee, Better thermoregulation of brain temperature using phase change material-mediated head cooling system, Int. J. Heat Mass Transf. 173 (2021) 121204, https://doi.org/10.1016/j.ijheatmasstransfer.2021.121204.
[15] Y. Jun, C.H. Park, H. Shim, T.J. Kang, Thermal Comfort Properties of Wearing Caps from Various Textiles, Text. Res. J. 79 (2) (2009) 179–189, https://doi.org/10.1177/0040517508093444.
[16] S.F. Neves, J.B.L.M. Campos, T.S. Mayor, Effects of clothing and fibres properties on the heat and mass transport, for different body heat/sweat releases, Appl. Therm. Eng. 117 (2017) 109–121, https://doi.org/10.1016/j.applthermaleng.2017.01.074.
[17] M. Junaid, G. Saha, P. Shahrear, S.C. Saha, Phase change material performance in chamfered dual enclosures: exploring the roles of geometry, inclination angles and heat flux, Int. J. Thermofluids 24 (2024) 100919, https://doi.org/10.1016/j.ijft.2024.100919.
[18] D. Nagaraju, B.V.N. Santhosi, A.R. Mohammad, J. Syed, N.K. Kolla, Numerical investigation of sustainable thermal energy storage (TES) system for personal helmet cooling, Int. J. Thermofluids 20 (2023) 100481.
[19] A. Rakotondrandisa, Doctoral dissertation, Normandie Université, 2019.
[20] M. Junaid, A.M.M. Mukaddes, M. Mahmud-Or-Rashid, Physical activities aid in tumor prevention: a finite element study of bio-heat transfer in healthy and malignant breast tissues, Heliyon 10 (14) (2024) e34650, https://doi.org/10.1016/j.heliyon.2024.e34650.
[21] B. Kamkari, H. Shokouhmand, F. Bruno, Experimental investigation of the effect of inclination angle on convection-driven melting of phase change material in a rectangular enclosure, Int. J. Heat Mass Transf. 72 (2014) 186–200, https://doi.org/10.1016/j.ijheatmasstransfer.2014.01.014.